EMBRY-RIDDLE
Aeronautical University™
SCHOLARLY COMMONS

Publications

5-1-2013

Influence of Microstructure on Thermoelastic Wave Propagation

Arkadi Berezovski
Tallinn University of Technology, arkadi.berezovski@cs.ioc.ee

Mihhail Berezovski
Worcester Polytechnic Institute, berezovm@erau.edu

Follow this and additional works at: https://commons.erau.edu/publication

Part of the Mechanics of Materials Commons, Numerical Analysis and Computation Commons, and the Partial Differential Equations Commons

Arkadi Berezovski · Mihhail Berezovski

Influence of microstructure on thermoelastic wave propagation

Abstract Numerical simulations of the thermoelastic response of a microstructured material on a thermal loading are performed in the one-dimensional setting to examine the influence of temperature gradient effects at the microstructure level predicted by the thermoelastic description of microstructured solids [14]. The system of equations consisting of a hyperbolic equation of motion, a parabolic macroscopic heat conduction equation, and a hyperbolic evolution equation for the microtemperature, is solved by a finite-volume numerical scheme. Effects of microtemperature gradients exhibit themselves on the macrolevel due to the coupling of equations of the macromotion and evolution equations for macro- and microtemperatures.

1 Introduction

The thermoelastic wave propagation suggests a coupling between elastic deformation and heat conduction [1]. However, the description of thermoelastic waves is usually restricted by the consideration of homogeneous solids [2] even for non-Fourier heat conduction laws [3–5]. At the same time, microstructure-oriented

A. Berezovski
Centre for Nonlinear Studies, Institute of Cybernetics at Tallinn University of Technology, Akadeemia tee 21, 12618 Tallinn, Estonia
Tel.: +372-462-04164
Fax: +372-462-04151
E-mail: Arkadi.Berezovski@cs.ioc.ee

M. Berezovski
Department of Mathematical Sciences, Worcester Polytechnic Institute, 100 Institute Rd, Worcester, MA, 01609, USA

theories of generalized continua [6–9] are, as a rule, isothermal. Attempts to include into consideration microstructural thermal effects [10,11] did not provide impressive results [12].

As it was noted by Tamma and Zhou [13], "experiments suggest that the wave type of temperature propagation is important for materials with nonhomogeneous inner structure". This means that temperature gradient effects at the microstructure level are expected to influence the thermomechanical response of a material. The corresponding theory has been proposed recently using the dual internal variables approach [14,15].

In the framework of this theory, the overall description of thermomechanical processes in microstructured solids includes both direct and indirect couplings of equations of motion and heat conduction at the macrolevel. In addition to the conventional direct coupling, there exists a coupling between the macromotion and the microtemperature evolution. This means that the macrodeformation can induce microtemperature perturbations due to the heterogeneity in the presence of a microstructure. These perturbations, propagating with a finite speed, can induce, in turn, corresponding changes in the macrotemperature. The appearing changes in the macrotemperature affect macrodeformations once more.

In what follows, predictions of the abovementioned theory are tested by numerical simulations of the thermoelastic response of a microstructured material on a thermal loading in the one-dimensional setting. For this purpose, the one-dimensional version of the theory is formulated first. Next, numerical scheme applied for the computations is described. Numerical results of a test problem are presented in the last part of the paper.

2 One-dimensional thermoelastic wave propagation in solids with microstructure

The behavior of materials depends on constitutive relations between state variables. The standard way to describe them is to specify explicitly the dependence of the free energy on state variables. In the framework of the dual internal variables approach [16], we suppose that the free energy depends on internal variables φ, ψ and their space derivatives $W = \overline{W}(u_x, \theta, \varphi, \varphi_x, \psi, \psi_x)$. We use a quadratic free energy function [14]

$$
\begin{aligned}
W = &\frac{1}{2}\left(\lambda + 2\mu\right)u_x^2 - \frac{\rho_0 c_p}{2\theta_0}\left(\theta - \theta_0\right)^2 + m\left(\theta - \theta_0\right)u_x + \\
&+ A\varphi u_x + A'\varphi_x u_x + \frac{1}{2}B\varphi^2 + \frac{1}{2}C\varphi_x^2 + \frac{1}{2}D\psi^2.
\end{aligned}
\tag{1}
$$

Here $u_x = \varepsilon$ is the one-dimensional strain measure, ρ_0 is the density, c_p is the heat capacity, the thermoelastic coefficient m is related to the dilatation coefficient α and the Lamé coefficients λ and μ by $m = -\alpha(3\lambda + 2\mu)$, θ_0 is the reference temperature, $A, A', B, C,$ and D are material parameters, subscripts denote derivatives.

This means that state variables include strain, temperature, and two internal variables (and their gradients). For simplicity, only a contribution of the second internal variable itself is included here. The corresponding constitutive relations

determine macrostress σ

$$\sigma := \frac{\partial \overline{W}}{\partial u_x} = (\lambda + 2\mu) u_x + m (\theta - \theta_0) + A\varphi + A'\varphi_x, \tag{2}$$

microstress η

$$\eta := -\frac{\partial \overline{W}}{\partial \varphi_x} = -C\varphi_x - A'u_x, \tag{3}$$

the interactive internal force τ

$$\tau := -\frac{\partial \overline{W}}{\partial \varphi} = -Au_x - B\varphi, \tag{4}$$

and auxilary quantities related to the second internal variable

$$\zeta = -\frac{\partial \overline{W}}{\partial \psi_x} = 0, \quad \xi = -\frac{\partial \overline{W}}{\partial \psi} = -D\psi. \tag{5}$$

The one-dimensional motion of the thermoelastic conductors of heat is governed by local balance laws for linear momentum and energy (no body forces)

$$(\rho_0 v)_t - \sigma_x = 0, \tag{6}$$

$$\left(\frac{1}{2}\rho_0 v^2 + E\right)_t - (\sigma v - Q)_x = 0, \tag{7}$$

and by the second law of thermodynamics

$$S_t + \left(\frac{Q}{\theta} + J\right)_x \geq 0. \tag{8}$$

Here v is the particle velocity, Q is the heat flux, E is the internal energy, S is the entropy, θ is temperature, J is the extra entropy flux.

In terms of the free energy per unit volume $W := E - S\theta$, the second law of thermodynamics results in the dissipation inequality

$$-(W_t + S\theta_t) + \sigma \varepsilon_t + (\theta J)_x - \left(\frac{Q}{\theta} + J\right)\theta_x \geq 0, \tag{9}$$

Introducing the non-zero extra entropy flux according to the procedure proposed by Maugin [17]

$$J = -\theta^{-1}\eta\varphi_t - \theta^{-1}\zeta\psi_t, \tag{10}$$

we reduce the dissipation inequality to the sum of intrinsic and thermal parts

$$\Phi = (\tau - \eta_x)\varphi_t + (\xi - \zeta_x)\psi_t - \left(\frac{Q - \eta\varphi_t - \zeta\psi_t}{\theta}\right)\theta_x \geq 0. \tag{11}$$

Assuming that the intrinsic dissipation is independent of the temperature gradient, we are forced to modify the Fourier law as follows

$$Q - \eta\varphi_t - \zeta\psi_t = -k\theta_x, \tag{12}$$

to satisfy the thermal part of the dissipation inequality.

The remaining intrinsic part of dissipation inequality (11) is satisfied by a choice of evolution equations for internal variables. As it is shown in [14], the thermal influence of a microstructure can be taken into account by the following choice

$$\varphi_t = R(\xi - \zeta_x), \quad \psi_t = -R(\tau - \eta_x) + R_2(\xi - \zeta_x). \tag{13}$$

where R and R_2 are certain appropriate constants. This choice leads to that the intrinsic dissipation is partly canceled and its remaining part is the square with a positive coefficient.

It follows from Eqs. (13) and (5) that

$$\varphi_t = -RD\psi, \tag{14}$$

i.e., the dual internal variable ψ is proportional to the time derivative of the primary internal variable φ_t. Then the evolution equation for the secondary internal variable

$$\psi_t = -R(\tau - \eta_x) + R_2(\xi - \zeta_x), \tag{15}$$

can be represented as

$$-\frac{1}{RD}\varphi_{tt} = -R(C\varphi_{xx} + A'u_{xx} - Au_x - B\varphi) + \frac{R_2}{R}\varphi_t, \tag{16}$$

or in the following form ($I = 1/R^2 D$)

$$I\varphi_{tt} + \frac{R_2}{R^2}\varphi_t = C\varphi_{xx} + A'u_{xx} - Au_x - B\varphi, \tag{17}$$

which is a Cattaneo-Vernotte-type hyperbolic equation [18] for the primary internal variable φ.

Correspondingly, energy conservation equation (7) in this case has the form

$$\rho_0 c_p \,\theta_t - \left(\kappa^2 \theta_x\right)_x = m\theta_0 u_{xt} + \frac{R_2}{R^2}\varphi_t^2, \tag{18}$$

where κ^2 is the thermal conductivity. Equation for macrotemperature (18) is influenced by a source term which depends on the internal variable φ.

Let us consider the case when the free energy depends only on the gradient of the primary internal variable, but not on the variable itself. This case corresponds to the choice of coefficients $A = 0, B = 0$ in Eq. (1). The corresponding equations of motion are coupled [14]

$$\rho_0 u_{tt} = (\lambda + 2\mu)\, u_{xx} + m\theta_x + A'\varphi_{xx}, \tag{19}$$

$$I\varphi_{tt} + \frac{R_2}{R^2}\varphi_t = (C\varphi_{xx} + A'u_{xx}), \tag{20}$$

which means that the primary internal variable possesses a wave-like behavior induced by the macrodeformation. Identifying the primary internal variable with the microtemperature [14], we see that the microtemperature may induce a wave-like propagation also for the macrotemperature due to the corresponding source term in heat conduction equation (18). Physically, the introduced microtemperature describes fluctuations about the mean temperature due to the presence of a microstructure.

3 Numerical scheme

In order to construct a numerical scheme for the solution of system of equations (18)-(20), it is convenient to represent governing equations in the form of a system of first-order partial differential equations. System of equations of motion for solids with microstructure (19), (20) can be rewritten using the notation

$$\varphi_t = w, \quad \varphi_x = \gamma, \tag{21}$$

as the system of first-order partial differential equations

$$\rho_0 v_t = \rho_0 c_0^2 \varepsilon_x + A' \gamma_x + m\theta_x, \tag{22}$$

$$\varepsilon_t = v_x, \tag{23}$$

$$I w_t = C\gamma_x + A' \varepsilon_x - R_2 R^{-2} w, \tag{24}$$

$$\gamma_t = w_x, \tag{25}$$

and complemented by energy conservation equation (18)

$$\rho_0 c_p \, \theta_t + q_x = m\theta_0 v_x + R_2 R^{-2} w^2, \tag{26}$$

where q is the Fourier heat flux, which is proportional to the temperature gradient

$$q(x,t) = -\kappa^2 \theta_x, \tag{27}$$

and $c_0 = \sqrt{(\lambda + 2\mu)/\rho_0}$ is the velocity of elastic wave.

We will solve system of Eqs. (21) - (27) numerically.

3.1 Local equilibrium approximation

Let us introduce a one-dimensional computational grid of cells $\mathcal{C}_n = [x_n, x_{n+1}]$ with interfaces $x_n = n\Delta x$ and time levels $t_k = k\Delta t$. For simplicity, the grid size Δx and the time step Δt are assumed to be constant. Each cell is considered as a thermodynamic system. Following the local equilibrium approximation [19], we introduce averaged and excess quantities in the computational cell both for macro- and microfields

$$\begin{aligned} \rho_0 c_0^2 \varepsilon = \bar{\sigma} + \Sigma, \quad v = \bar{v} + V, \quad \gamma = \bar{\gamma} + \Gamma, \\ w = \bar{w} + \Omega, \quad \theta = \bar{\theta} + \Theta, \quad q = \bar{q} + Q. \end{aligned} \tag{28}$$

Here overbars denote averaged quantities and capital letters correspond to excess quantities. Integrating Eqs. (22) - (26) over a computational cell, we have then, respectively,

$$\begin{aligned} \rho_0 \frac{\partial}{\partial t} \int_{x_n}^{x_{n+1}} v dx = \bar{\sigma}_n + \Sigma_n^+ - \bar{\sigma}_n - \Sigma_n^- + A'\bar{\gamma}_n + A'\Gamma_n^+ - A'\bar{\gamma}_n - A'\Gamma_n^- + \\ + m\bar{\theta}_n + m\Theta_n^+ - m\bar{\theta}_n - m\Theta_n^- = \Sigma_n^+ - \Sigma_n^- + A'\Gamma_n^+ - A'\Gamma_n^- + m\Theta_n^+ - m\Theta_n^-, \end{aligned} \tag{29}$$

$$\frac{\partial}{\partial t} \int_{x_n}^{x_{n+1}} \varepsilon dx = v_n^+ - v_n^- = \bar{v}_n + V_n^+ - \bar{v}_n - V_n^- = V_n^+ - V_n^-, \qquad (30)$$

$$I\frac{\partial}{\partial t} \int_{x_n}^{x_{n+1}} w dx = C(\bar{\gamma}_n + \Gamma_n^+) + \frac{A'}{\rho_0 c_0^2}(\bar{\sigma}_n + \Sigma_n^+) -$$

$$-C(\bar{\gamma}_n + \Gamma_n^-) - \frac{A'}{\rho_0 c_0^2}(\bar{\sigma}_n + \Sigma_n^-) - R_2 R^{-2} \bar{w}_n \Delta x = \qquad (31)$$

$$= C(\Gamma_n^+ - \Gamma_n^-) + \frac{A'}{\rho_0 c_0^2}(\Sigma_n^+ - \Sigma_n^-) - R_2 R^{-2} \bar{w}_n \Delta x,$$

$$\frac{\partial}{\partial t} \int_{x_n}^{x_{n+1}} \gamma dx = w_n^+ - w_n^- = \bar{w}_n + \Omega_n^+ - \bar{w}_n - \Omega_n^- = \Omega_n^+ - \Omega_n^-, \qquad (32)$$

$$\rho_0 c_p \frac{\partial}{\partial t} \int_{x_n}^{x_{n+1}} \theta dx = -\bar{q}_n - Q_n^+ + \bar{q}_n + Q_n^- + m\theta_0 \bar{v}_n + m\theta_0 V_n^+ - m\theta_0 \bar{v}_n - m\theta_0 V_n^-$$

$$+ R_2 R^{-2} \bar{w}_n^2 \Delta x = -Q_n^+ + Q_n^- + m\theta_0 V_n^+ - m\theta_0 V_n^- + R_2 R^{-2} \bar{w}_n^2 \Delta x. \qquad (33)$$

Here upper indices "+" and "-" of excess quantities denote their values at right and left ends of the cell, respectively.

The standard approximation of time derivatives in left hand sides of Eqs. (29) - (33) leads to the numerical scheme in terms of excess quantities

$$\rho_0 \bar{v}_n^{k+1} - \rho_0 \bar{v}_n^k = \frac{\Delta t}{\Delta x}\left(\Sigma_n^+ - \Sigma_n^-\right) + A'\frac{\Delta t}{\Delta x}\left(\Gamma_n^+ - \Gamma_n^-\right) + m\frac{\Delta t}{\Delta x}\left(\Theta_n^+ - \Theta_n^-\right) \quad (34)$$

$$\bar{\varepsilon}_n^{k+1} - \bar{\varepsilon}_n^k = \frac{\Delta t}{\Delta x}\left(V_n^+ - V_n^-\right). \qquad (35)$$

$$I\bar{w}_n^{k+1} - I\bar{w}_n^k = \frac{C\Delta t}{\Delta x}\left(\Gamma_n^+ - \Gamma_n^-\right) + \frac{A'}{\rho_0 c_0^2}\frac{\Delta t}{\Delta x}(\Sigma_n^+ - \Sigma_n^-) - R_2 R^{-2}\bar{w}_n \Delta t \qquad (36)$$

$$\bar{\gamma}_n^{k+1} - \bar{\gamma}_n^k = \frac{\Delta t}{\Delta x}\left(\Omega_n^+ - \Omega_n^-\right), \qquad (37)$$

$$\rho_0 c_p \bar{\theta}_n^{k+1} - \rho_0 c_p \bar{\theta}_n^k = -\frac{\Delta t}{\Delta x}\left(Q_n^+ - Q_n^-\right) + \frac{m\theta_0 \Delta t}{\Delta x}\left(V_n^+ - V_n^-\right) + R_2 R^{-2}\bar{w}_n^2 \Delta t \qquad (38)$$

because the averaged quantities are defined by

$$\bar{v} = \frac{1}{\Delta x}\int_{x_n}^{x_{n+1}} v dx, \quad \bar{\varepsilon} = \frac{1}{\Delta x}\int_{x_n}^{x_{n+1}} \varepsilon dx, \quad \bar{\theta} = \frac{1}{\Delta x}\int_{x_n}^{x_{n+1}} \theta dx,$$

$$\bar{w} = \frac{1}{\Delta x}\int_{x_n}^{x_{n+1}} w dx, \quad \bar{\gamma} = \frac{1}{\Delta x}\int_{x_n}^{x_{n+1}} \gamma dx. \qquad (39)$$

The next step is the calculation of excess quantities.

3.2 Excess quantities

The values of excess quantities at the boundaries between cells are determined from jump relations

$$
\begin{aligned}
&[[\rho_0 c_0^2 \varepsilon + A'\gamma + m\theta]] = 0, \\
&[[v]] = 0, \\
&[[C\gamma + A'\varepsilon]] = 0, \\
&[[w]] = 0, \\
&[[\theta]] = 0,
\end{aligned}
\tag{40}
$$

which express the continuity of full stresses, temperatures, and velocities across stationary discontinuities at the micro- and macroscale.

First four jump relations (40) can be represented at each boundary between neighboring cells as

$$
\Sigma_{n+1}^- - \Sigma_n^+ + A'\Gamma_{n+1}^- - A'\Gamma_n^+ = -(\rho_{n+1}c_{n+1}^2\bar{\varepsilon}_{n+1} - \rho_n c_n^2 \bar{\varepsilon}_n) - A'(\bar{\gamma}_{n+1} - \bar{\gamma}_n),
\tag{41}
$$

$$
V_{n+1}^- - V_n^+ = -(\bar{v}_{n+1} - \bar{v}_n),
\tag{42}
$$

$$
C\Gamma_{n+1}^- - C\Gamma_n^+ + \frac{A'}{\rho_{n+1}c_{n+1}^2}\Sigma_{n+1}^- - \frac{A'}{\rho_n c_n^2}\Sigma_n^+ = -(C\bar{\gamma}_{n+1} - C\bar{\gamma}_n) - (\bar{\varepsilon}_{n+1} - \bar{\varepsilon}_n),
\tag{43}
$$

$$
\Omega_{n+1}^- - \Omega_n^+ = -(\bar{w}_{n+1} - \bar{w}_n).
\tag{44}
$$

However, the jump relations provide only four relations between eight introduced dynamic excess quantities. Remaining dependencies follow from the Riemann invariants conservation [22]

$$
\rho_0 c_0 V_n^- + \Sigma_n^- \sqrt{1 + \frac{A'}{\rho_0 c_0^2}} = 0,
\tag{45}
$$

$$
\rho_0 c_0 V_{n-1}^+ - \Sigma_{n-1}^+ \sqrt{1 - \frac{A'}{\rho_0 c_0^2}} = 0,
\tag{46}
$$

$$
\Omega_n^- + c_1 \Gamma_n^- \sqrt{1 + \frac{A'}{Ic_1^2}} = 0,
\tag{47}
$$

$$
\Omega_{n-1}^+ - c_1 \Gamma_{n-1}^+ \sqrt{1 - \frac{A'}{Ic_1^2}} = 0,
\tag{48}
$$

where a characteristic velocity for the microstructure, c_1, is introduced as $C = Ic_1^2$.

It is also instructive to represent the continuity of temperature in a numerical form. For example, at the left boundary of the computational cell we have

$$
\bar{\theta}_{n-1} + \left(\Theta^+\right)_{n-1} = \bar{\theta}_n + \left(\Theta^-\right)_n.
\tag{49}
$$

Assuming the symmetry of heat conduction in the homogenized body

$$\left(\Theta^+\right)_{n-1} = -\left(\Theta^-\right)_n, \tag{50}$$

we can calculate temperature excesses as follows:

$$\left(\Theta^+\right)_{n-1} = \frac{1}{2}\left(\bar{\theta}_n - \bar{\theta}_{n-1}\right), \tag{51}$$

$$\left(\Theta^-\right)_n = -\frac{1}{2}\left(\bar{\theta}_n - \bar{\theta}_{n-1}\right), \tag{52}$$

and the difference between excess temperatures at the right and left sides of a computational cell is

$$\left(\Theta^+\right)_n - \left(\Theta^-\right)_n = \frac{1}{2}\left(\bar{\theta}_{n+1} - \bar{\theta}_{n-1}\right). \tag{53}$$

Now we turn to the Fourier heat flux

$$q(x,t) = -\kappa^2 \frac{\partial \theta}{\partial x}. \tag{54}$$

Integration Eq. (54) over the computational cell leads to

$$\int_{x_n}^{x_{n+1}} q\,dx = -\kappa^2 \theta_n^+ + \kappa^2 \theta_n^- = -\kappa^2(\bar{\theta}_n + \Theta_n^+ - \bar{\theta}_n - \Theta_n^-) = -\kappa^2(\Theta_n^+ - \Theta_n^-). \tag{55}$$

The latter means that the average value of the Fourier heat flux is determined by the difference of the temperature excess at the boundaries of the same computational cell

$$\bar{q}_n = \frac{1}{\Delta x}\int_{x_n}^{x_{n+1}} q\,dx = -\frac{\kappa^2}{\Delta x}(\Theta_n^+ - \Theta_n^-). \tag{56}$$

The heat flux excess is assumed to be continuous

$$[\![Q]\!] = 0, \tag{57}$$

and is determined by the difference of the temperature excess at the boundary of neighboring computational cells

$$Q_{n-1}^+ = Q_n^- = \frac{\kappa^2}{\Delta x}(\Theta_n^- - \Theta_{n-1}^+). \tag{58}$$

The latter relation allows us to calculate the heat flux excess difference

$$Q_n^+ - Q_n^- = \frac{\kappa^2}{\Delta x}(\Theta_{n+1}^- - \Theta_n^+ - \Theta_n^- + \Theta_{n-1}^+). \tag{59}$$

Due to the continuity of temperature we can represent the difference in terms of averaged temperatures

$$Q_n^+ - Q_n^- = \frac{\kappa^2}{\Delta x}(\bar{\theta}_n - \bar{\theta}_{n+1} - \bar{\theta}_{n-1} + \bar{\theta}_n) = -\frac{\kappa^2}{\Delta x}(\bar{\theta}_{n+1} + \bar{\theta}_{n-1} - 2\bar{\theta}_n). \tag{60}$$

Equations (41) - (48), (51), (52), and (58) allow to calculate all excess quantities algebraically. The constructed numerical scheme is a necessary extension of the thermoelastic wave propagation algorithm, that was successfully applied for the two-dimensional thermoelastic wave propagation in media with rapidly-varying properties [20–22].

4 Numerical simulations

The main purpose of numerical simulations is the comparison of the response of materials with and without microstructure on a thermal loading.

4.1 Initial and boundary conditions

We consider a thermoelastic half-space occupying the region $x \geq 0$. It is assumed that the half-space is initially at rest. This means that values of all the fields are equal to zero at the initial time instant. Boundary conditions prescribe values of macroscopic fields (like strain, stress, velocity, temperature) at the boundary plane. Especially, we are interested in a thermal loading (non-zero temperature). Therefore, we assume that the traction free boundary plane is heated for the first 100 time steps following the rule

$$\bar{\theta}(0,t) = \frac{1}{2}\left(1 + cos\left(\frac{\pi(t - 50\Delta t)}{50}\right)\right),\tag{61}$$

which forms a heat pulse at the boundary plane.

4.2 Computed fields and parameters identification

The averaged fields

$$\bar{v}, \quad \bar{\varepsilon}, \quad \bar{w}, \quad \bar{\gamma}, \quad \bar{\theta},\tag{62}$$

are computed by means of Eqs. (34) - (38). The corresponding excess quantities

$$V^{\pm}, \quad \Sigma^{\pm}, \quad \Omega^{\pm}, \quad \Gamma^{\pm}, \quad \Theta^{\pm},\tag{63}$$

are calculated by means of Eqs. (41) - (48), (51), (52), and (58), respectively.

To perform the computations, we need to prescribe the values of material and geometry parameters of the problem. It is clear that parameters of the macromotion $\rho_0, c_0, \theta_0, m, c_p, k$ follow the choice of material, L is the macroscopic characteristic length (a size of the computational domain), U_0 is the size of excitation, I is the mass fraction of the material which constitutes the microstructure, and c_1 is the corresponding elastic wave velocity. Only three parameters, namely, a', c' and R_2/R^2 are model parameters and may be adjusted.

The macroscopic properties of the material are chosen similar to that for titanium: $\rho_0 = 4510$ kg/m^3, $c_0 = 5240$ m/s, whereas properties of the microstructure material is similar to that for aluminium: $I = 2703$ kg/m^3, $c_1 = 5020$ m/s. The scale of excitation, U_0, is chosen as 100 times less than the macroscopic length, L, so that $U_0/L = 0.01$. The scale of the microstructure, l, is comparable with the scale of excitation $l/L = 0.0128$. The reference temperature is chosen as $\theta_0 = 300^0 C$, and the thermoelastic coefficient, m, corresponds to the choice $m\theta_0 = -0.1\rho_0 c_0^2$. The heat capacity, c_p, is chosen in such a way that $c_p\theta_0 = c_1 c_0 10^{-9}$. It is assumed that the thermal conductivity is rather small ($\kappa^2 = 0.0001 L c_0 \rho_0 c_p$). The model parameters used in calculations had the following values:

$$\frac{R_2 l}{R^2 \rho_0 c_0} = 0.02, \quad A' = 0.03\rho_0 c_0^2, \quad C = 0.1\rho_0 c_0^2.\tag{64}$$
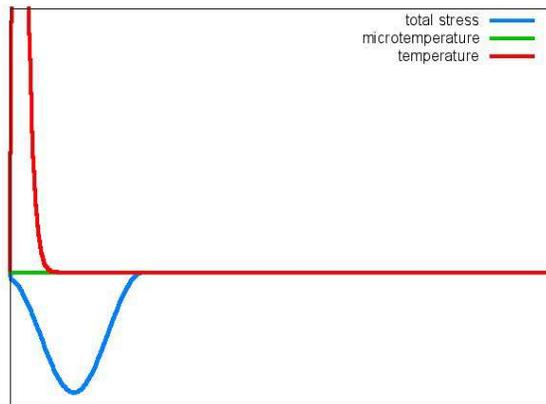
Fig. 1 Distribution of temperature, stress, and microtemperature in a homogeneous half-space at 100 time steps.
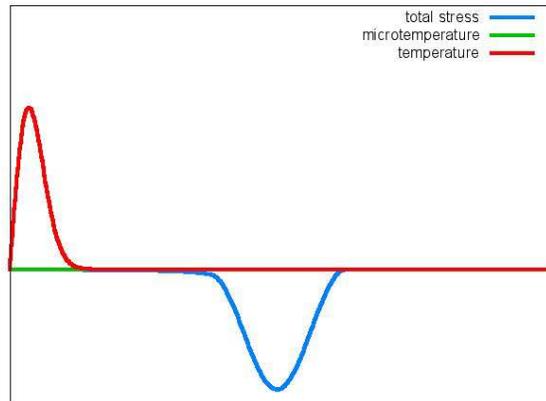

Fig. 2 Distribution of temperature, stress, and microtemperature in a homogeneous half-space at 250 time steps.

The choice of model parameters completes the description of the problem.

4.3 Results and discussion

Computations were performed separately for the homogeneous thermoelastic half-space (without microstructure) and for the half-space with a microstructure. Results of calculations of temperature and stress distribution along the x-axis in a homogeneous half-space at different instants of time are presented in Figs. 1–3. In this classical thermal stress problem, the temperature pulse is diffused slowly near the heat source at the left boundary, whereas an induced stress wave is formed and
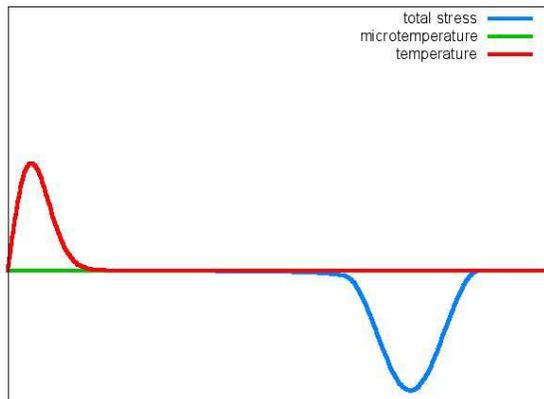
Fig. 3 Distribution of temperature, stress, and microtemperature in a homogeneous half-space at 350 time steps.
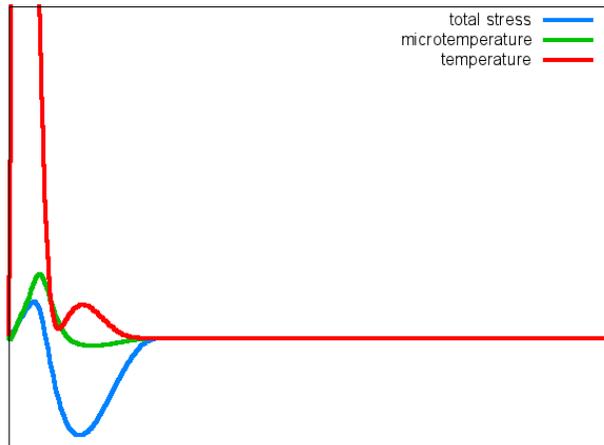

Fig. 4 Distribution of temperature, stress, and microtemperature in a microstructured half-space at 100 time steps.

propagated along the x-axis without dispersion. The microtemperature is equal to zero. It should be noted that the amplitudes of temperature and stress are normalized in such a way that they can be presented in the same figure. Therefore, there is no legend along the axes.

Calculations of the same problem with the microstructure modeling are presented in Figs. 4–6. Again, the pulse of macrotemperature is slowly diffused and the induced stress wave is propagated along the x-axis. Additionally, a microtemperature pulse is induced by the stress wave, which, in its turn, produces a wave-like behavior of the macrotemperature. The stress wave is slightly distorted by the microstructure influence.
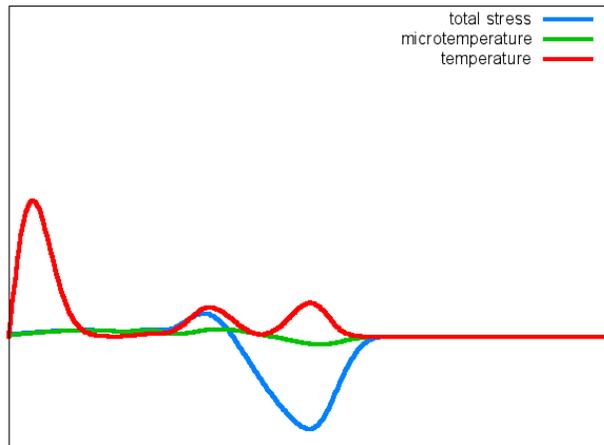
Fig. 5 Distribution of temperature, stress, and microtemperature in a microstructured half-space at 250 time steps.
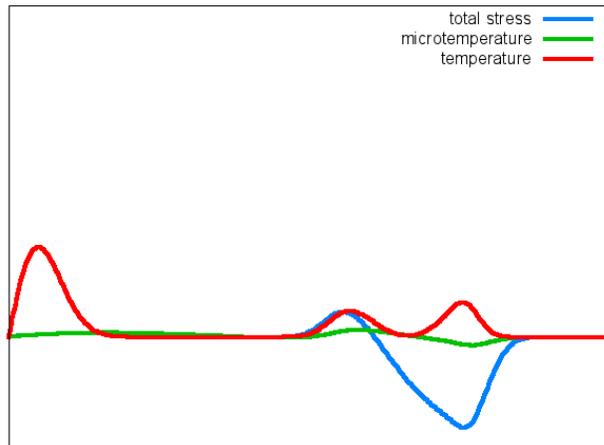

Fig. 6 Distribution of temperature, stress, and microtemperature in a microstructured half-space at 350 time steps.

Combined pictures of temperature and stress fields (Figs. 4–6) demonstrate that besides a parabolic type of the macroscopic heat conduction, the wave-like propagation of thermal fluctuations can be provided by the influence of microtemperature gradients. This influence, which is described by means of internal variables, manifests itself due to the coupling of equations governing the thermoelastic wave propagation. Thus, numerical simulations of thermoelastic wave propagation in solids with microstructure show that it is not necessary to introduce a hyperbolic heat conduction equation for the macrotemperature to observe its wave-like behavior. As one can see, thermal gradients produced by an appropriate microstructure are able to generate these fluctuations propagating with a finite speed.

References

1. Nowacki, W.: Thermoelasticity. Pergamon Press, Oxford (1962)
2. Hetnarski, R.B., Reza Eslami, M.: Thermal Stresses – Advanced Theory and Applications. Springer, Berlin (2009)
3. Chandrasekharaiah, D.S.: Hyperbolic thermoelasticity: a review of recent literature. Appl. Mech. Rev. **51**, 705–729 (1998)
4. Hetnarski, R.B., Ignaczak. J.: Generalized thermoelasticity. J. Thermal Stresses **22**, 451–476 (1999)
5. Ignaczak, J., Ostoja-Starzewski, M.: Thermoelasticity with Finite Wave Speeds. Oxford University Press, Oxford, UK (2010)
6. Mindlin, R.D.: Micro-structure in linear elasticity. Arch. Rat. Mech. Anal. **16** 51–78 (1964)
7. Capriz, G.: Continua with Microstructure. Springer, Heidelberg (1989)
8. Eringen, A.C.: Microcontinuum Field Theories. vol.I. Springer, New York (1999)
9. Forest, S.: Micromorphic approach for gradient elasticity, viscoplasticity, and damage. J. Eng. Mech. **13**, 117–131 (2009)
10. Cardona, J.-M., Forest, S., Sievert, R.: Towards a theory of second grade thermoelasticity. Extracta Math. **14**, 127–140 (1999)
11. Forest, S., Amestoy, M.: Hypertemperature in thermoelastic solids. C. R. Mecanique **336**, 347–353 (2008)
12. Nguyen, Q.-S.: On standard dissipative gradient models. Ann. Solid Struct. Mech. **1**, 79–86 (2010)
13. Tamma, K.K., Zhou, X.: Macroscale and microscale thermal transport and thermo-mechanical interactions: some noteworthy perspectives. J. Thermal Stresses **21**, 405–449 (1998)
14. Berezovski, A., Engelbrecht, J., Maugin, G.A.: Thermoelasticity with dual internal variables. J. Thermal Stresses **34**, 413–430 (2011)
15. Berezovski, A., Engelbrecht, J.: Waves in microstructured solids: dispersion and thermal effects. In: Bai, Y., Wang, J., Fang, D., (eds.) Proceedings of the 23rd International Congress of Theoretical and Applied Mechanics, August 19 - 24, 2012, Beijing, China, CD-ROM, SM07-005 (2012)
16. Ván, P., Berezovski, A., Engelbrecht, J.: Internal variables and dynamic degrees of freedom. J. Non-Equilib. Thermodyn. **33**, 235–254 (2008)
17. Maugin, G.A.: Internal variables and dissipative structures. J. Non-Equilib. Thermodyn. **15**, 173–192 (1990)
18. Joseph, D.D., Preziosi, L.: Heat waves. Rev. Mod. Phys. **61**, 41–73 (1989)
19. Muschik, W., Berezovski, A.: Thermodynamic interaction between two discrete systems in non-equilibrium. J. Non-Equilib. Thermodyn. **29**, 237–255 (2004)
20. Berezovski, A., Maugin, G.A.: Simulation of thermoelastic wave propagation by means of a composite wave-propagation algorithm. J. Comp. Physics **168**, 249–264 (2001)
21. Berezovski, A., Maugin, G.A.: Thermoelastic wave and front propagation. J. Thermal Stresses **25**, 719–743 (2002)
22. Berezovski, A., Engelbrecht, J., Maugin, G.A.: Numerical Simulation of Waves and Fronts in Inhomogeneous Solids. World Scientific, Singapore (2008)